Random fields from quenched disorder in an archetype for correlated electrons: The parallel spin stripe phase of $La_{1.6-x}Nd_{0.4}Sr_xCuO_4$ at the 1/8 anomaly

Q. Chen[1,2] S. H.-Y. Huang[1] Q. Ma[1] E. M. Smith[1] H. Sharron[1] A. A. Aczel[3] W. Tian[3] and B. D. Gaulin[1,2,4]

[1]*Department of Physics and Astronomy, McMaster University, Hamilton, Ontario, Canada L8S 4M1*
[2]*Brockhouse Institute for Materials Research, Hamilton, Ontario, Canada L8S 4M1*
[3]*Neutron Scattering Division, Oak Ridge National Laboratory, Oak Ridge, Tennessee 37831, USA*
[4]*Canadian Institute for Advanced Research, Toronto, Ontario, Canada M5G 1M1*

The parallel stripe phase is remarkable both in its own right, and in relation to the other phases with which it coexists. Its inhomogeneous nature makes such states susceptible to random fields from quenched magnetic vacancies. We argue this is the case by introducing low concentrations of nonmagnetic Zn impurities (0%–10%) into $La_{1.6-x}Nd_{0.4}Sr_xCuO_4$ (Nd-LSCO) with $x = 0.125$ in single-crystal form, well below the percolation threshold of ∼41% for a two-dimensional square lattice. Elastic neutron scattering measurements on these crystals show clear magnetic quasi-Bragg peaks at all Zn dopings. While all the Zn-doped crystals display order parameters that merge into each other and the background at ∼68 K, the temperature dependence of the order parameter as a function of Zn concentration is drastically different. This result is consistent with meandering charge stripes within the parallel stripe phase, which are pinned in the presence of quenched magnetic vacancies. In turn it implies vacancies that preferentially occupy sites within the charge stripes, and hence that can be very effective at disrupting superconductivity in Nd-LSCO ($x = 0.125$), and, by extension, in all systems exhibiting parallel stripes.

Parallel stripe order and fluctuations have been proposed to underlie the mechanism for high-T_c superconductivity in layered copper oxides [1–7]. This unusual, inhomogeneous, intertwined spin and charge structure is described in terms of narrow strips of antiphase Néel states that are separated from each other by charge stripes, as illustrated in Fig. 1. The parallel spin stripe phase in the cuprates is the strongest in $La_{1.6-x}Nd_{0.4}Sr_xCuO_4$ (Nd-LSCO) at the "1/8 anomaly" ($x = 0.125$) [8,9], where its onset temperature was thought to maximize at ∼50 K, and its superconducting T_c is at a local minimum [10–12]. The parallel charge stripes are observed at twice the incommensurate wave vectors of the spin stripes, and were thought to have a somewhat higher-temperature onset [8]. Together, these intertwined parallel spin and charge orders have been consistently interpreted in terms of the parallel stripe picture which possesses a remarkable *inhomogeneous* magnetic structure. This inhomogeneous magnetic structure has been observed to coexist with superconductivity in Nd-LSCO, from $x = 0.05$ to $x = 0.26$ [13–20]. However, whether stripes help or hinder superconductivity remains a matter of debate.

Other than the collinear stripe picture [3,21–24], the incommensurate magnetic peaks observed in the cuprates are also discussed in terms of spiral spin density wave (SDW) states caused by Fermi-surface nesting [25–28]. This inherently itinerant origin for a form of spiral magnetism does *not* require inhomogeneity. In principle, neutron crystallographic techniques should be able to distinguish between inhomogeneous stripe and homogeneous spiral SDW structures, but the complexity of the relevant spin structures make this problem difficult [24].

The subject of this paper is the sensitivity of the parallel stripe phase to quenched disorder. It is interesting precisely because the parallel stripe phase possesses an inhomogeneous magnetic structure with a nonmagnetic sublattice, and therefore quenched disorder is expected to couple to this structure as a random field. In fact, quenched disorder in the form of magnetic vacancies has been well studied in the parent compound, quasi-two-dimensional (2D) quantum antiferromagnet La_2CuO_4, by jointly substituting Zn and Mg on the Cu site [29]. This neutron scattering work shows beautifully how quenched disorder in this related but *homogeneous* magnetic structure, a simple two-sublattice Néel state, gives rise to the expectations of the 2D percolation theory—a percolation threshold of ∼41% [30].

Inhomogeneous magnetic structures are relatively rare in nature, but can occur, for example, in the presence of geometrical frustration in insulators. One well-studied example is that of the stacked triangular lattice antiferromagnet $CsCoBr_3$, which comprises triangular layers of antiferromagnetically coupled Ising Co^{2+} magnetic moments, which are then stacked on top of each other to form a three-dimensional structure. This material displays three phase transitions and three magnetically ordered states as a function of temperature in zero magnetic field, with a high-temperature ordered phase which is "partially paramagnetic." Within this structure, the three sublattices making up the triangular plane are occupied by Co^{2+} spins which are up, down, and paramagnetic. It is therefore a long-range ordered structure where one of the sublattices making up the structure is itself disordered. At lower temperatures, weak interactions beyond near-neighbor exchange, allow the paramagnetic sublattice to order, but

134411-1

FIG. 1. A schematic drawing of parallel stripe order in the La214 cuprate with quenched nonmagnetic Zn impurities replacing Cu in the CuO$_2$ plane. Only the Cu sites are shown. This 2D parallel stripe structure is an inhomogeneous arrangement of holes (solid gray circles), and spins (arrows) within a CuO$_2$ plane, while the open circles represent paramagnetic sites. Shading of the arrowheads distinguishes the antiphase Néel domains.
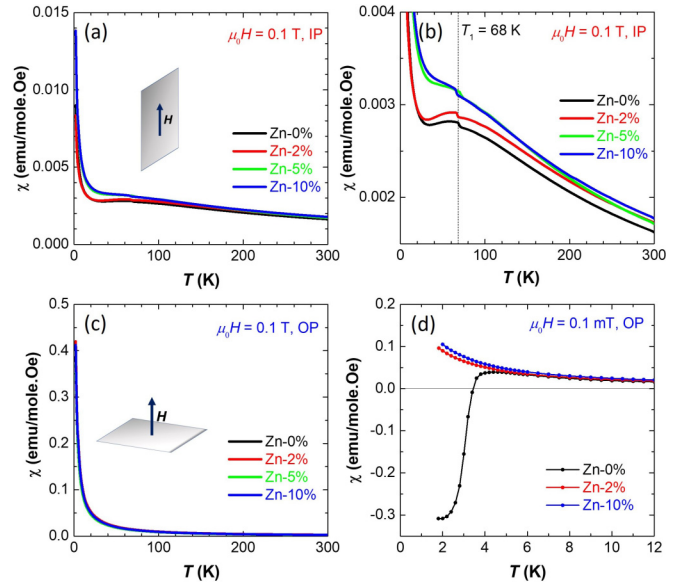

FIG. 2. Magnetic susceptibility measurements for Zn-doped single crystals of Nd-LSCO ($x = 0.125$) with field (a), (b) in-plane (IP) and (c), (d) out-of-plane (OP). (a) and (b) show the same data on different scales. (c) and (d) show field OP measurements with 0.1 T and 0.1 mT, respectively. The insets in (a) and (c) illustrate the orientation of the CuO$_2$/ab plane of the crystals relative to the external field.

an inhomogeneous, partially paramagnetic structure exists over an extended range of temperature at intermediate temperatures [31]. Neutron diffraction studies on single-crystal CsCo$_{0.83}$Mg$_{0.17}$Br$_3$ by van Duijn *et al.* [32] showed that quenched magnetic vacancies (Mg^{2+} substituting for Co^{2+}) severely disrupt the nature of the magnetic order parameter in this system, over the temperature range of the inhomogeneous, partially paramagnetic phase. The extreme sensitivity of the magnetic order parameter to the quenched magnetic vacancies is attributed to the random field Ising model (RFIM) behavior. Upon Mg doping, the system enters a RFIM domain state and only orders at sufficiently low temperatures.

We propose that very similar phenomena could occur in the parallel stripe phase of the cuprates. The pinning of nonmagnetic charge stripes by quenched magnetic vacancies within the parallel stripe structure is qualitatively illustrated in Fig. 1. This figure shows a Zn concentration of ~6%, which causes fluctuations in the parallel spin stripe width. The charge stripes follow the local pattern of quenched Zn impurities to minimize the magnetic exchange interaction energy of a Zn impurity, compared with when the impurity is located within the middle of a Néel domain. Although wider charge stripes are possible [5,33,34], they are abstracted to being a single Cu site across in Fig. 1. The key characteristic of the charge stripe is that the parallel spin stripes on either side of it are antiphase Néel states, π out of phase relative to each other, thus giving rise to the incommensurate nature of the magnetic Bragg peaks. In what follows we focus on the Nd-LSCO family at 1/8 doping, and present experimental evidence for this picture, and discuss implications for the nature of superconducting pairing in this, and by extension, many phases of cuprate superconductors.

High-quality single crystals of Zn-doped Nd-LSCO ($x = 0.125$) were grown using the traveling solvent floating zone technique [12,35,36]. Magnetization was measured on sin-

gle crystals using a Quantum Design magnetic properties measurement system (MPMS) superconducting quantum interference device (SQUID) magnetometer. Elastic neutron scattering measurements were performed with the fixed-incident-energy triple-axis spectrometer HB-1A at Oak Ridge National Laboratory.

Magnetic susceptibilities were measured to characterize the magnetic/charge order [Figs. 2(a)–2(c)] and superconducting [Fig. 2(d)] transitions. The zero-field-cooled (ZFC) warm-up, followed by field-cooled (FC) cool-down measurement protocols were employed. For clarity, only FC data are shown because the ZFC and FC data overlap, except for the Zn-0% sample measured at 0.1 mT, which shows the ZFC-FC bifurcation near the superconducting transition and is consistent with previous studies [10,12].

The $H \parallel ab$ (IP) measurements in Figs. 2(a) and 2(b) show a discontinuity at $T_1 \sim 68$ K, coincident with the low-temperature-orthorhombic (LTO) to low-temperature-tetragonal (LTT) structural phase transition [12]. A broad peak, roughly centered at T_1, suggests the onset of strong antiferromagnetic fluctuations in the parallel spin stripe phases. While the field-IP data below ~100 K show systematic Zn dependence, in contrast, the $H \parallel c$ (OP) data in Fig. 2(c) are almost Zn independent, likely due to the large random moments of Nd^{3+} whose crystal field effects maintain their orientation along the c axis. In Fig. 2(d), the low-temperature measurements for the Zn-0% sample show a sharp drop below $T_c \sim 3$ K, while no signs of superconducting transition are observed down to 1.8 K for the other samples. This result, that 2% of nonmagnetic Zn impurities suppress T_c by a factor of at least 2, is consistent with previous studies of Zn doping in La$_{2-x}$Ba$_x$CuO$_4$ (LBCO), La$_{2-x}$Sr$_x$CuO$_4$ (LSCO),
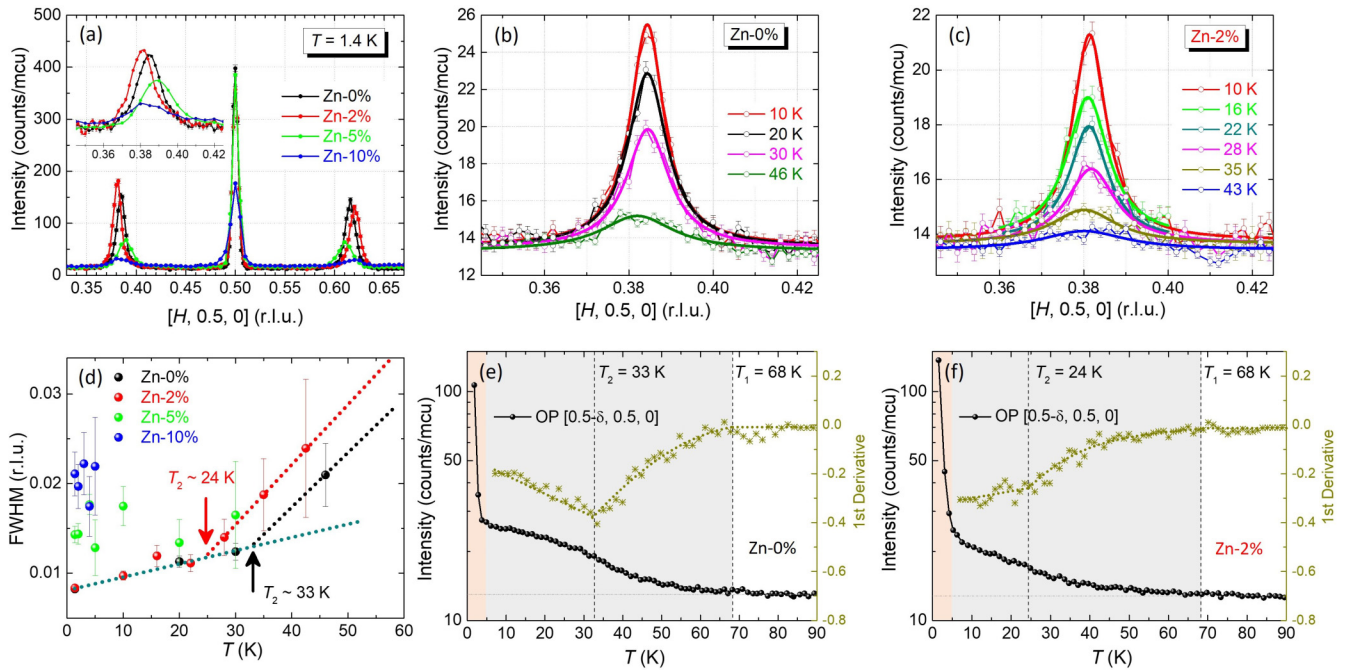
FIG. 3. (a) Elastic neutron scattering scans of the form $[H, 0.5, 0]$ near $H = 0.5$ at 1.4 K. The inset shows the same intensities at $H = 0.5 - \delta$ on log intensity scale. (b), (c) Elastic H scans through $[0.5 - \delta, 0.5, 0]$ for Zn-0% and Zn-2% samples at different temperatures. These data have been fit to Lorentzian line shapes (solid lines). (d) FWHM extracted from these fits as a function of temperature. (e), (f) Order parameter of the $[0.5 - \delta, 0.5, 0]$ ($\delta \approx 0.125$) magnetic peak for Zn-0% and Zn-2%, respectively. Anomalies in the first derivative derived from these order parameters allow us to estimate $T_2 \sim 33(1)$ and 24(2) K for Zn-0% and Zn-2%, respectively. The dashed lines are guides to the eyes.

$YBa_2Cu_3O_{7-x}$ (YBCO), and Nd-LSCO systems, where the suppression of T_c by nonmagnetic Zn is described with the "swiss cheese" model wherein charge carriers within an area of $\pi \xi_{ab}^2$ around each Zn are excluded from the superfluid, where ξ_{ab} is the in-plane coherence length [37–44].

Our elastic neutron scattering studies of the incommensurate magnetic Bragg peaks associated with the parallel spin stripe phase used $E_i = 14.5$ meV. A collimation of $40' - 40' - 40' - 80'$ resulted in an energy resolution at the elastic line just over 1 meV [full width at half maximum (FWHM)]. The single-crystal samples were mounted so that the $(HK0)$ peaks are in the scattering plane, where HKL are defined in tetragonal notation with $a \simeq 3.78$ Å and $c \simeq 13.14$ Å.

Elastic neutron scattering scans of the form $[H, 0.5, 0]$ and $[0.5, K, 0]$ near $H(K) = 0.5$ were carried out for all four single crystals. Figure 3(a) shows the data measured at base temperature $T = 1.4$ K. Only H scans are shown because they overlap with the corresponding K scans. Incommensurate antiferromagnetic quasi-Bragg peaks are observed at $[0.5 \pm \delta, 0.5, 0]$ and $[0.5, 0.5 \pm \delta, 0]$, with $\delta \approx 0.125$ at all Zn dopings. Commensurate nuclear Bragg peaks are observed at $[0.5, 0.5, 0]$, between the incommensurate antiferromagnetic quasi-Bragg peaks. The temperature dependence of this commensurate nuclear scattering is sensitive to the structural LTO to LTT phase transition at $T_1 \sim 68$ K.

The inset of Fig. 3(a) shows the comparison of the $[0.5 - \delta, 0.5, 0]$ peaks on a log intensity scale. The peak intensity varies by a factor of ~ 9 between the Zn-0% and the Zn-10% samples, and the high Zn-doped single crystals clearly exhibit quasi-Bragg peaks which are broader in the $(HK0)$ plane. In

addition, shifts in the peak position of up to 0.004 r.l.u. in H can be seen. These shifts are not systematic with Zn doping, and are likely due to a small, random variation in the Sr or hole concentration of single crystals by ± 0.004, assuming that the wave vector follows the Yamada relation $\delta \approx x$ [45].

The order parameter of the incommensurate wave vector $[0.5 - \delta, 0.5, 0]$ for the Zn-0% and 2% samples is shown in Figs. 3(e) and 3(f), respectively. Our data for the pure sample (Zn-0%) are very similar to that originally reported [8], but with better counting statistics and a much increased temperature-point density, allowing a sensitive measurement of the form of the order parameter.

At the lowest temperatures, below 5 K, one sees a dramatic upturn in the order parameter, which was ascribed to the effect of coupling between the Nd^{3+} moments randomly distributed over the La^{3+} sites between the CuO_2 planes, to the Cu^{2+} moments within the plane [9]. Such coupling is known to develop three-dimensional (3D) correlations into the parallel spin stripe phase, which are absent above ~ 5 K. This effect concentrates the elastic incommensurate magnetic scattering at $[0.5 - \delta, 0.5, 0]$, as opposed to along the line $[0.5 - \delta, 0.5, L]$. This strong, quasi-3D parallel spin stripe order coexists perfectly well with superconductivity below T_c.

Above 5 K, the order parameter for Zn-0% shows typical behavior, with a downward curvature approaching what appears to be a phase transition near $T_2 \sim 33$ K. The quality of the order parameter data for the Zn-0% and Zn-2% samples in Figs. 3(e) and 3(f) is sufficiently high that it can be fit to a polynomial expansion such that the first derivative of the order parameter can also be obtained as a function of temperature.
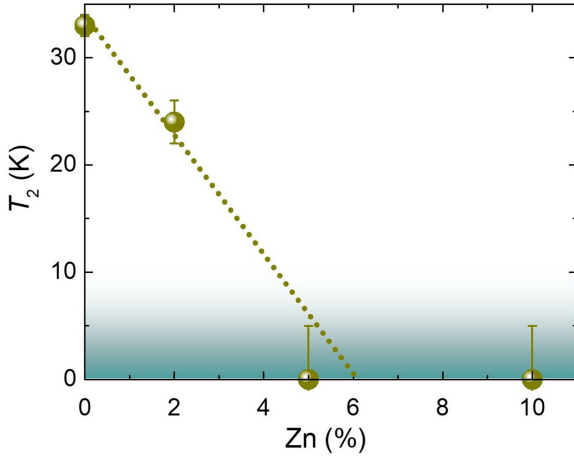
FIG. 4. The spin stripe transition temperature T_2 for Nd-LSCO ($x = 0.125$) as a function of Zn concentration, as identified by elastic neutron scattering order parameter measurements. The shaded temperature region below ∼7 K indicates temperatures below which coupling between the Nd^{3+} and Cu^{2+} moments strongly influences the stripe structure.
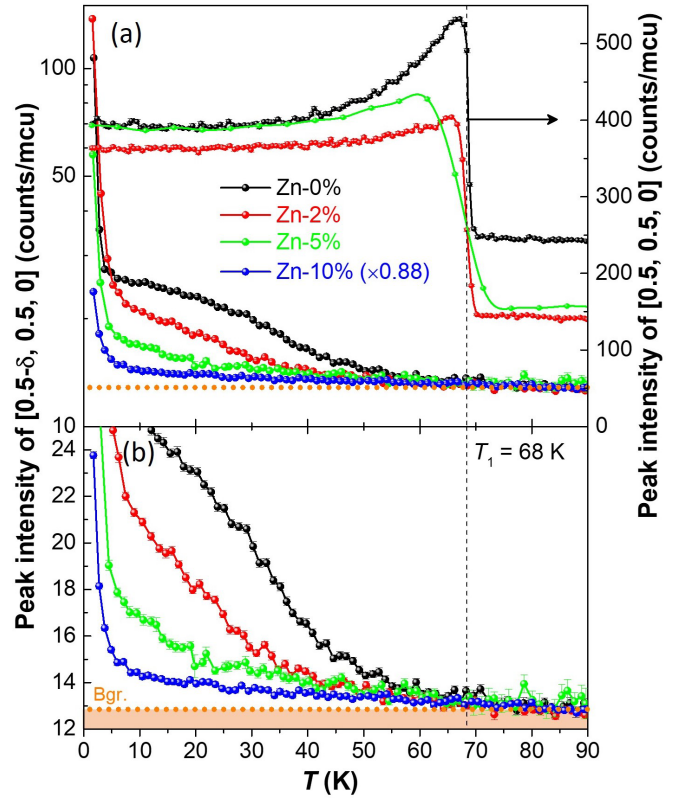

FIG. 5. The order parameters of Nd-LSCO ($x = 0.125$) single crystals with four different Zn-doping concentrations on both log and linear intensity scales. The intensity of the Zn-10% sample has been multiplied by 0.88 in order to have the intensity for all four samples agree for $T > T_1$, but otherwise the intensities are normalized only to the beam monitor count unit (mcu). (a) also shows the temperature dependence of the commensurate nuclear Bragg peak at [0.5, 0.5, 0].

This is shown in Figs. 3(e) and 3(f) on the right-hand scale. For Zn-0% in Fig. 3(e), a sharp change in slope is observed at $T_2 = 33(1)$ K, where the order parameter changes from an upward curvature to downward curvature. A similar feature is observed at $T_2 = 24(2)$ K for Zn-2% in Fig. 3(f). Note that $T_2 \sim 30$ K has been previously identified as the onset temperature for static magnetism in pure Nd-LSCO ($x = 0.125$) by muon spin relaxation/rotation (μSR) studies [43,46].

The incommensurate peaks of the parallel spin stripe order are clearly observed above T_2 for both Zn-0% and 2% samples as seen in Figs. 3(b) and 3(c), and order parameter intensity is observed up until $T_1 \sim 68$ K for both samples, before its slope goes to zero. The corresponding charge stripe order in Nd-LSCO ($x = 0.125$) is known to onset below ∼68 K as well [8,9,47–49]. Our present results clearly show that both spin and charge stripes onset at *the same* temperature.

The elastic line scans in Figs. 3(b) and 3(c) have been fit to Lorentzian line shapes to extract widths related to correlation lengths in the *ab* plane as a function of temperature. The so-extracted FWHM are plotted in Fig. 3(d), and both show a linearly decreasing correlation length (increasing FWHM) at temperatures below $T_2 \sim 33$ and 24 K for the Zn-0% and 2% crystals, respectively. Above T_2, the slope of the decreasing correlation lengths with increasing temperature increases. The same Lorentzian analysis for Zn-5% and Zn-10% crystals is also done and included in the Appendix in Fig. 6. Despite the larger error bar associated with the FWHM for the Zn-5% and Zn-10% samples, we can see that near 2 K, the widths are larger for the higher Zn-doped crystals. This indicates two things: The parallel spin stripe phases in Zn-0% and 2% doped Nd-LSCO ($x = 0.125$) samples do not display true long-range order down to 1.4 K, consistent with earlier results [50]; and a transition of sorts occurs at $T_2 \approx 33$ K (24 K) for the Zn-0% (Zn-2%) samples. The transition at T_2 may simply be where the ordered moment participating in the parallel spin stripe structure begins to saturate. As mentioned above, μSR, a

local probe, detects moments which are static on the muon timescale at T_2 in pure Nd-LSCO ($x = 0.125$) [43,46]. But finite correlation lengths within the basal *ab* plane exist much below T_2, while the correlation length along *c* is short for all temperatures above 5 K [9]. Hence T_2 may be a crossover temperature scale on which the low-energy spin dynamics rapidly evolve and pass through the μSR time window.

For Zn-5% and 10% single crystals, as will be discussed, the much-weaker order parameters at high Zn doping show an upward curvature at all temperatures above 1.4 K, hence consistent with $T_2 \sim 0$. The T_2's extracted from this analysis on all four Nd-LSCO single-crystal samples are shown in Fig. 4, and the extreme sensitivity of the parallel spin stripe phase to quenched magnetic vacancies is evident as T_2 appears to be suppressed to zero by Zn-6%, almost a factor of 7 below the 2D percolation threshold of ∼41%.

A previous μSR and neutron study by Guguchia *et al.* [43] on La214 cuprate systems showed that the spin stripe order temperature T_{so} responded similarly to Zn doping as that of T_2 which we obtain by neutron scattering, shown in Fig. 4. However, the only neutron diffraction data reported in that earlier study, the order parameter of Nd-LSCO ($x = 0.125$) with Zn-1.6% doping, shows this order parameter goes to zero at $T_{so} \approx 10$ K, a result which is inconsistent with our order parameter
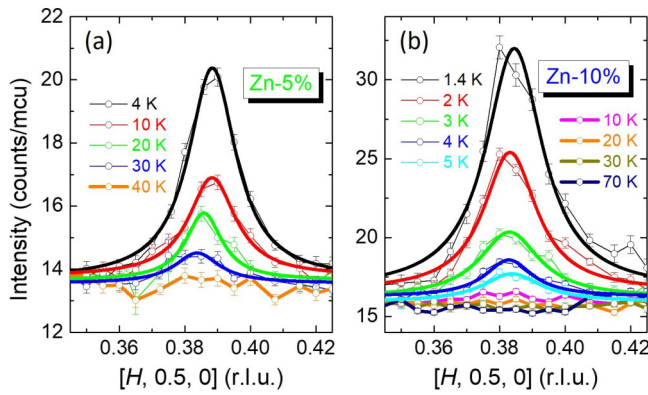
FIG. 6. Elastic H scans through $[0.5 - \delta, 0.5, 0]$ for Zn-5% and Zn-10% samples at different temperatures. These data have been fit to Lorentzian line shapes (solid lines). FWHM extracted from these fits are shown in Fig. 3(d).

for Nd-LSCO ($x = 0.125$) with Zn-2% in Figs. 3(f), 4, and 5, and with our $[0.5 - \delta, 0.5, 0]$ line scans above 10 K for the same Zn-2% sample as shown in Fig. 3(c). Nonetheless, our present elastic neutron scattering results and Guguchia *et al.*'s μSR results lead to a very similar and striking sensitivity of parallel spin stripe phase to quenched nonmagnetic disorder. Guguchia *et al.*'s work also showed that superconducting T_c possesses a similar Zn-doping sensitivity for LSCO and LBCO near optimal doping for superconductivity.

We then summarize the full order parameters of all four Zn-doped Nd-LSCO ($x = 0.125$) single crystals in Fig. 5 on both log and linear intensity scales, respectively. Figure 5(a) also shows the temperature dependence of the commensurate nuclear Bragg peak at $[0.5, 0.5, 0]$. Its abrupt drop in intensity at T_1 signals the LTT to LTO structural phase transition, which broadens slightly with increasing Zn doping, but does not significantly move in temperature. The decrease in its intensity just below the LTT transition to ~40 K is observed, possibly related to a secondary structural transition, but the exact transition requires further crystallographic investigation. The parallel spin stripe order parameters are severely and systematically affected by the Zn doping from Zn-2% to 10%, despite the fact that they are all well below the 2D percolation threshold of ~41%. At 5% and 10% Zn doping, the peak intensity of the parallel spin stripe quasi-Bragg peak is sufficiently weak that a well-defined peak, similar to what is shown in Figs. 3(b) and 3(c), is not easily identifiable above 10 K.

This is shown in the Appendix in Fig. 6. As discussed, the Zn-5% and Zn-10% order parameters show upward curvatures at all temperatures.

This is very reminiscent of the order parameter for $CsCo_{0.83}Mg_{0.17}Br_3$, in the temperature regime for the partially paramagnetic Néel state displayed by pure $CsCoBr_3$. It was attributed to the quenched impurities coupling to the inhomogeneous Néel state as a random field [32]. A similar interpretation is relevant here, again due to an inhomogeneous ordered state—in this case the parallel stripe phase. The similarity between the two is very striking, and RFIM provides a natural framework for understanding our results, although the parallel stripe phase is more complicated and involves itinerant carriers, while the former is insulating.

This is an interesting conclusion for at least three reasons. First, it presents a rare example of a systematic study of random field effects from quenched disorder in an inhomogeneous ordered magnetic state. Second, it provides strong evidence that the incommensurate, ordered structure below ~50 K in Nd-LSCO ($x = 0.125$) and related La214 cuprates is an *inhomogeneous* parallel spin stripe phase and not a *homogeneous* spiral SDW. Third, and perhaps most importantly, it implies that quenched nonmagnetic impurities are preferentially located coincident with the parallel charge stripe component of the parallel stripe structure, as the parallel charge stripes will seek them out to lower the magnetic energy of the inhomogeneous parallel stripe structure. Quenched magnetic vacancies can therefore be very effective at breaking up Cooper pairs propagating along the charge stripes, and can thereby account for the extreme sensitivity of the superconducting T_c to nonmagnetic disorder in the CuO_2 plane in Nd-LSCO ($x = 0.125$), and by extension in other cuprate superconductors for which an inhomogeneous stripe phase is relevant.

APPENDIX: ADDITIONAL DATA

Additional Q-scan data and a Lorentzian peak line-shape analysis for the higher Zn-doped crystals (Zn-5% and Zn-10%) are shown in Fig. 6.

[1] V. J. Emery, S. A. Kivelson, and O. Zachar, Spin-gap proximity effect mechanism of high-temperature superconductivity, Phys. Rev. B **56**, 6120 (1997).

[2] S. A. Kivelson, E. Fradkin, and V. J. Emery, Electronic liquid-crystal phases of a doped Mott insulator, Nature (London) **393**, 550 (1998).

[3] S. A. Kivelson, I. P. Bindloss, E. Fradkin, V. Oganesyan, J. M. Tranquada, A. Kapitulnik, and C. Howald, How to detect fluctuating stripes in the high-temperature superconductors, Rev. Mod. Phys. **75**, 1201 (2003).

[4] E. W. Huang, C. B. Mendl, S. Liu, S. Johnston, H.-C. Jiang, B. Moritz, and T. P. Devereaux, Numerical evidence of fluctuating stripes in the normal state of high-T_c cuprate superconductors, Science **358**, 1161 (2017).

[5] J. M. Tranquada, Cuprate superconductors as viewed through a striped lens, Adv. Phys. **69**, 437 (2020).

[6] H.-C. Jiang and S. A. Kivelson, Stripe order enhanced superconductivity in the Hubbard model, Proc. Natl. Acad. Sci. USA **119**, e2109406119 (2022).

[7] H. Xu, C.-M. Chung, M. Qin, U. Schollwöck, S. R. White, and S. Zhang, Coexistence of superconductivity with partially filled stripes in the Hubbard model, arXiv:2303.08376.

[8] J. M. Tranquada, B. J. Sternlieb, J. D. Axe, Y. Nakamura, and S. Uchida, Evidence for stripe correlations of spins and holes in copper oxide superconductors, Nature (London) **375**, 561 (1995).

[9] J. M. Tranquada, J. D. Axe, N. Ichikawa, Y. Nakamura, S. Uchida, and B. Nachumi, Neutron scattering study of stripe-phase order of holes and spins in $La_{1.48}Nd_{0.4}Sr_{0.12}CuO_4$, Phys. Rev. B **54**, 7489 (1996).

[10] J. D. Axe and M. K. Crawford, Structural instabilities in lanthanum cuprate superconductors, J. Low Temp. Phys. **95**, 271 (1994).

[11] B. Michon, C. Girod, S. Badoux, J. Kačmarčík, Q. Ma, M. Dragomir, H. A. Dabkowska, B. D. Gaulin, J.-S. Zhou, S. Pyon, T. Takayama, H. Takagi, S. Verret, N. Doiron-Leyraud, C. Marcenat, L. Taillefer, and T. Klein, Thermodynamic signatures of quantum criticality in cuprate superconductors, Nature (London) **567**, 218 (2019).

[12] M. Dragomir, Q. Ma, J. P. Clancy, A. Ataei, P. A. Dube, S. Sharma, A. Huq, H. A. Dabkowska, L. Taillefer, and B. D. Gaulin, Materials preparation, single-crystal growth, and the phase diagram of the cuprate high-temperature superconductor $La_{1.6-x}Nd_{0.4}Sr_xCuO_4$, Phys. Rev. Mater. **4**, 114801 (2020).

[13] S.-W. Cheong, G. Aeppli, T. E. Mason, H. Mook, S. M. Hayden, P. C. Canfield, Z. Fisk, K. N. Clausen, and J. L. Martinez, Incommensurate magnetic fluctuations in $La_{2-x}Sr_xCuO_4$, Phys. Rev. Lett. **67**, 1791 (1991).

[14] T. E. Mason, G. Aeppli, and H. A. Mook, Magnetic dynamics of superconducting $La_{1.86}Sr_{0.14}CuO_4$, Phys. Rev. Lett. **68**, 1414 (1992).

[15] T. R. Thurston, P. M. Gehring, G. Shirane, R. J. Birgeneau, M. A. Kastner, Y. Endoh, M. Matsuda, K. Yamada, H. Kojima, and I. Tanaka, Low-energy incommensurate spin excitations in superconducting $La_{1.85}Sr_{0.15}CuO_4$, Phys. Rev. B **46**, 9128 (1992).

[16] S. Wakimoto, J. M. Tranquada, T. Ono, K. M. Kojima, S. Uchida, S.-H. Lee, P. M. Gehring, and R. J. Birgeneau, Diagonal static spin correlation in the low-temperature orthorhombic *Pccn* phase of $La_{1.55}Nd_{0.4}Sr_{0.05}CuO_4$, Phys. Rev. B **64**, 174505 (2001).

[17] M. Fujita, H. Goka, K. Yamada, J. M. Tranquada, and L. P. Regnault, Stripe order, depinning, and fluctuations in $La_{1.875}Ba_{0.125}CuO_4$ and $La_{1.875}Ba_{0.075}Sr_{0.050}CuO_4$, Phys. Rev. B **70**, 104517 (2004).

[18] R. J. Birgeneau, C. Stock, J. M. Tranquada, and K. Yamada, Magnetic neutron scattering in hole-doped cuprate superconductors, J. Phys. Soc. Jpn. **75**, 111003 (2006).

[19] Q. Ma, K. C. Rule, Z. W. Cronkwright, M. Dragomir, G. Mitchell, E. M. Smith, S. Chi, A. I. Kolesnikov, M. B. Stone, and B. D. Gaulin, Parallel spin stripes and their coexistence with superconducting ground states at optimal and high doping in $La_{1.6-x}Nd_{0.4}Sr_xCuO_4$, Phys. Rev. Res. **3**, 023151 (2021).

[20] Q. Ma, E. M. Smith, Z. W. Cronkwright, M. Dragomir, G. Mitchell, A. I. Kolesnikov, M. B. Stone, and B. D. Gaulin, Dynamic parallel spin stripes from the 1/8 anomaly to the end

of superconductivity in $La_{1.6-x}Nd_{0.4}Sr_xCuO_4$, Phys. Rev. Res. **4**, 013175 (2022).

[21] M. Charlebois, S. Verret, A. Foley, O. Simard, D. Sénéchal, and A.-M. S. Tremblay, Hall effect in cuprates with an incommensurate collinear spin-density wave, Phys. Rev. B **96**, 205132 (2017).

[22] H. J. Schulz, Incommensurate antiferromagnetism in the two-dimensional Hubbard model, Phys. Rev. Lett. **64**, 1445 (1990).

[23] M. Fleck, A. I. Lichtenstein, and A. M. Oleś, Spectral properties and pseudogap in the stripe phases of cuprate superconductors, Phys. Rev. B **64**, 134528 (2001).

[24] N. B. Christensen, H. M. Rønnow, J. Mesot, R. A. Ewings, N. Momono, M. Oda, M. Ido, M. Enderle, D. F. McMorrow, and A. T. Boothroyd, Nature of the magnetic order in the charge-ordered cuprate $La_{1.48}Nd_{0.4}Sr_{0.12}CuO_4$, Phys. Rev. Lett. **98**, 197003 (2007).

[25] B. I. Shraiman and E. D. Siggia, Spiral phase of a doped quantum antiferromagnet, Phys. Rev. Lett. **62**, 1564 (1989).

[26] V. N. Kotov and O. P. Sushkov, Spiral spin order and transport anisotropy in underdoped cuprates, AIP Conf. Proc. **816**, 112 (2006).

[27] H. Yamase, A. Eberlein, and W. Metzner, Coexistence of incommensurate magnetism and superconductivity in the two-dimensional Hubbard model, Phys. Rev. Lett. **116**, 096402 (2016).

[28] A. Eberlein, W. Metzner, S. Sachdev, and H. Yamase, Fermi surface reconstruction and drop in the Hall number due to spiral antiferromagnetism in high-T_c cuprates, Phys. Rev. Lett. **117**, 187001 (2016).

[29] O. P. Vajk, P. K. Mang, M. Greven, P. M. Gehring, and J. W. Lynn, Quantum impurities in the two-dimensional spin one-half Heisenberg antiferromagnet, Science **295**, 1691 (2002).

[30] M. E. J. Newman and R. M. Ziff, Efficient Monte Carlo algorithm and high-precision results for percolation, Phys. Rev. Lett. **85**, 4104 (2000).

[31] M. Mao, B. D. Gaulin, R. B. Rogge, and Z. Tun, Tricritical behavior in a stacked triangular lattice Ising antiferromagnet $CsCoBr_3$, Phys. Rev. B **66**, 184432 (2002).

[32] J. van Duijn, B. D. Gaulin, M. A. Lumsden, J. P. Castellan, and W. J. L. Buyers, Random fields and the partially paramagnetic state of $CsCo_{0.83}Mg_{0.17}Br_3$: Critical scattering study, Phys. Rev. Lett. **92**, 077202 (2004).

[33] J. M. Tranquada, Spins, stripes, and superconductivity in hole-doped cuprates, AIP Conf. Proc. **1550**, 114 (2013).

[34] J. M. Tranquada, M. P. M. Dean, and Q. Li, Superconductivity from charge order in cuprates, J. Phys. Soc. Jpn. **90**, 111002 (2021).

[35] J.-Q. Yan, J.-S. Zhou, and J. B. Goodenough, Thermal conductivity in the stripe-ordered phase of cuprates and nickelates, Phys. Rev. B **68**, 104520 (2003).

[36] Q. Ma, E. M. Smith, Z. W. Cronkwright, M. Dragomir, G. Mitchell, B. W. Winn, T. J. Williams, and B. D. Gaulin, Magnetic field tuning of parallel spin stripe order and fluctuations near the pseudogap quantum critical point in $La_{1.36}Nd_{0.4}Sr_{0.24}CuO_4$, Phys. Rev. B **106**, 214427 (2022).

[37] B. Nachumi, A. Keren, K. Kojima, M. Larkin, G. M. Luke, J. Merrin, O. Tchernyshöv, Y. J. Uemura, N. Ichikawa, M. Goto, and S. Uchida, Muon spin relaxation studies of Zn-substitution effects in high-T_c cuprate superconductors, Phys. Rev. Lett. **77**, 5421 (1996).

[38] Y. Fukuzumi, K. Mizuhashi, K. Takenaka, and S. Uchida, Universal superconductor-insulator transition and T_c depression in Zn-substituted high-T_c cuprates in the underdoped regime, Phys. Rev. Lett. **76**, 684 (1996).

[39] T. Nakano, N. Momono, T. Nagata, M. Oda, and M. Ido, Contrasting Ni- and Zn-substitution effects on magnetic properties and superconductivity in La$_{2-x}$Sr$_x$CuO$_4$, Phys. Rev. B **58**, 5831 (1998).

[40] T. Adachi, S. Yairi, K. Takahashi, Y. Koike, I. Watanabe, and K. Nagamine, Muon spin relaxation and magnetic susceptibility studies of the effects of nonmagnetic impurities on the Cu spin dynamics and superconductivity in La$_{2-x}$Sr$_x$Cu$_{1-y}$Zn$_y$O$_4$ around $x = 0.115$, Phys. Rev. B **69**, 184507 (2004).

[41] P. M. Lozano, G. D. Gu, J. M. Tranquada, and Q. Li, Experimental evidence that zinc impurities pin pair-density-wave order in La$_{2-x}$Ba$_x$CuO$_4$, Phys. Rev. B **103**, L020502 (2021).

[42] J. Wen, Z. Xu, G. Xu, Q. Jie, M. Hücker, A. Zheludev, W. Tian, B. L. Winn, J. L. Zarestky, D. K. Singh, T. Hong, Q. Li, G. Gu, and J. M. Tranquada, Probing the connections between superconductivity, stripe order, and structure in La$_{1.905}$Ba$_{0.095}$Cu$_{1-y}$Zn$_y$O$_4$, Phys. Rev. B **85**, 134512 (2012).

[43] Z. Guguchia, B. Roessli, R. Khasanov, A. Amato, E. Pomjakushina, K. Conder, Y. J. Uemura, J. M. Tranquada, H. Keller, and A. Shengelaya, Complementary response of static spin-stripe order and superconductivity to nonmagnetic impurities in cuprates, Phys. Rev. Lett. **119**, 087002 (2017).

[44] Y. J. Uemura, G. M. Luke, B. J. Sternlieb, J. H. Brewer, J. F. Carolan, W. N. Hardy, R. Kadono, J. R. Kempton, R. F. Kiefl, S. R. Kreitzman, P. Mulhern, T. M. Riseman, D. L. Williams, B. X. Yang, S. Uchida, H. Takagi, J. Gopalakrishnan, A. W. Sleight, M. A. Subramanian, C. L. Chien *et al.*, Universal correlations between T_c and $\frac{n_s}{m^*}$ (carrier density over effective mass) in high-T_c cuprate superconductors, Phys. Rev. Lett. **62**, 2317 (1989).

[45] K. Yamada, C. H. Lee, K. Kurahashi, J. Wada, S. Wakimoto, S. Ueki, H. Kimura, Y. Endoh, S. Hosoya, G. Shirane, R. J. Birgeneau, M. Greven, M. A. Kastner, and Y. J. Kim, Doping dependence of the spatially modulated dynamical spin correlations and the superconducting-transition temperature in La$_{2-x}$Sr$_x$CuO$_4$, Phys. Rev. B **57**, 6165 (1998).

[46] B. Nachumi, Y. Fudamoto, A. Keren, K. M. Kojima, M. Larkin, G. M. Luke, J. Merrin, O. Tchernyshyov, Y. J. Uemura, N. Ichikawa, M. Goto, H. Takagi, S. Uchida, M. K. Crawford, E. M. McCarron, D. E. MacLaughlin, and R. H. Heffner, Muon spin relaxation study of the stripe phase order in La$_{1.6-x}$Nd$_{0.4}$Sr$_x$CuO$_4$ and related 214 cuprates, Phys. Rev. B **58**, 8760 (1998).

[47] J. M. Tranquada, J. D. Axe, N. Ichikawa, A. R. Moodenbaugh, Y. Nakamura, and S. Uchida, Coexistence of, and competition between, superconductivity and charge-stripe order in La$_{1.6-x}$Nd$_{0.4}$Sr$_x$CuO$_4$, Phys. Rev. Lett. **78**, 338 (1997).

[48] J. Takeda, T. Inukai, and M. Sato, Electronic specific heat of (La, Nd)$_{2-x}$Sr$_x$Cu$_{1-y}$Zn$_y$O$_4$ up to about 300 K, J. Phys. Chem. Solids **62**, 181 (2001).

[49] N. K. Gupta, C. McMahon, R. Sutarto, T. Shi, R. Gong, H. I. Wei, K. M. Shen, F. He, Q. Ma, M. Dragomir, B. D. Gaulin, and D. G. Hawthorn, Vanishing nematic order beyond the pseudogap phase in overdoped cuprate superconductors, Proc. Natl. Acad. Sci. USA **118**, e2106881118 (2021).

[50] J. M. Tranquada, N. Ichikawa, and S. Uchida, Glassy nature of stripe ordering in La$_{1.6-x}$Nd$_{0.4}$Sr$_x$CuO$_4$, Phys. Rev. B **59**, 14712 (1999).